Iranian Journal of Science and Technology, Transactions of Civil Engineering
https://doi.org/10.1007/s40996-022-00844-7

RESEARCH PAPER

Flow in Open and Closed Rectangular Channels with Moving Walls

Mahmoud F. Maghrebi[1] · **Abbas R. Moghaddam**[1]

Received: 19 February 2021 / Accepted: 5 February 2022

Abstract
In many situations, such as flows passing through a section of the channel widths, the sudden opening of the flow duct either on the horizon plane or on the vertical plane, there is a possibility of reverse flow. Couette Flow, which is flowing in channels with moving walls that move in opposite directions, can simulate these types of flows. For the first time, it is attempted to obtain and draw velocity contours and depth-averaged velocities in a rectangular channel with moving walls. The walls move at equal velocities and opposite directions to each other. This is done for channels with varying width-to-depth ratios. It is predicted that velocity contours and depth-averaged velocities will be very similar to the Couette flow between the two plates when the channel depth is greater than the width. The proposed model is used for this purpose by Maghrebi (Adv Water Resour 29:1504–1514, 2006. https://doi.org/10.1016/j.advwatres.2005.11.007). To simulate reverse flow, it is sufficient to consider the shear stresses direction on the walls to be in opposite directions to each other. The linear stress distribution is the best assumption to consider the shear stress distribution for the channel bed situated between the two walls. In this case, a hypothetical boundary is formed perpendicular to the middle of the cross section of the channel bed. It flows on both sides of the boundary having equal velocities but different signs. One of the interesting points in this phenomenon is drawing dimensionless isovel contour. The zero average velocity at the channel cross-section results from zero average discharge. Large amounts of dimensionless isovel contour occur in the vicinity of the moving walls that is difficult to imagine how the isovel contours were formed.

Keywords Couette flow · Isovel contour · Distribution of shear stress · Moving walls

1 Introduction

The flow characteristics in a recirculation zone are three-dimensional, and many experiments have been performed to identify the flow behavior in the recirculation zone (Dey and Barbhuiya 2005). Complexity in tidal current with the partial reverse flow is high because, in this case, two different parts of flow with positive and negative signs can be distinguished at any one time (Maghrebi and Givehchi 2010).

Investigating the velocity distribution profile in the Couette flow is one of the essential parts of the Couette flow analysis. The shear stresses of the walls during the Couette flow play an essential role in the relationships of the velocity distribution profile in the Couette flow. As long as the shear stresses in the Couette flow are constant, the shear stress gradients have no effect on the flow, and thus the Reynolds number effect in the Couette flow is seen (Kitoh et al. 2005). Hu et al. (2016) performed experimental and numerical simulations to reverse flow phenomenon in reverse U tube steam generators (UTSGs). When the reverse flow occurs, the negative pressure drops between the inlet and outlet plenums and the heat transfer of the UTSG reduce significantly.

In both Poiseuille and Couette flows, the friction coefficient and the overall kinetic energy decrease with increasing Reynolds number. In particular, the friction coefficient is approximately the same for the two flows when data are made non-dimensional concerning the centerline properties, supporting the wall law's universality. However, suppose the friction curve is reported as a function of the bulk properties. In that case, it is found that Couette flow yields less resistance than Poiseuille flow, probably up to a very high Reynolds number for a given mass flow rate. Similar behavior is observed for the integrated kinetic energy, which

✉ Mahmoud F. Maghrebi
maghrebi@um.ac.ir

Abbas R. Moghaddam
ab.rezaeimoghaddam@um.ac.ir

[1] Civil Engineering Department, Ferdowsi University of Mashhad, 91775-1111 Mashhad, Iran

Published online: 26 February 2022

abruptly changes from zero to a maximum corresponding to the transition threshold. These observations suggest the possible use of devices based on moving belts for fluid transport to minimize frictional losses and the effectiveness of Couette flows at low Reynolds number in promoting turbulent diffusion (Orlandi et al., 2015).

Pereira et al. (2017) provide direct numerical solutions to the Navier–Stokes time-dependent three-dimensional equations to evolve the three-dimensional finite-amplitude perturbations of the Poisson plane and Couette plate planes. It is found that plane Poiseuille flow can sustain neutrally stable two-dimensional finite-amplitude disturbances at Reynolds numbers more significant than about 2800. No neutrally stable two-dimensional finite-amplitude disturbances of plane Couette flow were found. Three-dimensional disturbances are shown to have a robust destabilizing effect. It is shown that finite-amplitude disturbances can drive the transition to turbulence in plane Poiseuille flow and plane Couette flow at Reynolds numbers of order 1000. Details of the resulting flow fields are presented. It is also shown that plane Poiseuille flow cannot sustain turbulence at Reynolds numbers below 500.

Shinneeb et al. (2021), in their studies, numerically investigate the effect of aspect on the velocity field characteristics of the turbulent flow of a straight open-channel flow. The transient three-dimensional Navier–Stokes equations were numerically solved using a finite-volume approach with an improved–delayed detached-eddy simulation turbulence model. The results revealed the formation of a pair of counter-rotating recirculation zones near the bottom corners of the channel, whose axes are aligned with the main flow direction. Each pair consists of a mean recirculation zone near the bed (bed recirculation zone), and another one near the sidewall (side recirculation zone).

Grosse and Schröder (2009) evaluated the distribution of shear stresses in the ducts with the turbulent flow by micro-Pillar sensors. Based on the results of these studies, the coexistence and overlap of areas with low shear stresses and areas with high shear stresses, traces of coherent structures near the walls are evident. They also observed that areas with low shear stresses are like long meandering bands intersected by areas with high shear stresses.

Telbany and Reynolds (1980) found that the slope of the central part of the velocity distribution profile depends mainly on the Reynolds number and the central 40% of the channel. The average shear stresses and the intensity of the turbulence are almost uniform. Liu et al. (2019) showed that extreme events occurring near the walls (such as reverse flow) are detected and analyzed based on the shear stress patterns of the walls. The few reverse flows identified by the distribution of wall shear stress at different Reynolds numbers are used as an empirical example of near-wall return current events in a turbulent flow.

Hafeez and Ndikilar (2014) discussed the steady laminar flow in incompressible viscous fluids between two porous parallel plates, which is suction in the upper plate and injection in the bottom plate. In this case, the flow is driven by a pressure gradient and a uniform vertical flow is created, and the vertical velocity is uniform throughout the flow field. They also discussed a solution for low and high Reynolds numbers and plotted velocity profile diagrams for the flow between two porous parallel plates. The upper plate is suction and in the bottom plate is injection.

Nasif et al. (2020) employed a numerical investigation in this study to evaluate the influence of channel aspect ratio varying between 2.0 and 12.0 on the secondary currents and other flow characteristics in an open-channel turbulent flow at mildly supercritical Froude numbers. It is shown that the streamwise velocity profile across the channel has a strong dependence on the channel aspect ratio. This profile has two recognizable inflection points for aspect ratios between 3.0 and 6.0, which move toward the sidewalls as the channel aspect ratio increases. A region of inviscid-like flow is seen about the central channel plane above a specific vertical location for a small channel aspect ratio only. The distribution of the contour patterns of mean vertical and transverse secondary currents is similar for a wide range. It does not depend on the channel aspect ratio.

In their studies, Hamilton et al. (1995) used a direct numerical simulation of a very limited Couette flow to study the dynamics of structures near the turbulent flow walls. They find that the computational domain dimensions reach the minimum values that stabilize the turbulence with the onset of a fully developed turbulent flow. A defined, quasi-cyclic, orderly trend is observed in the structures close to the walls. Komminaho et al. (1996) performed direct numerical simulation of turbulent Couette flow at Reynolds number 750. In their studies, they paid particular attention to selecting a large computing box that would accommodate even the most large-scale perturbations. Similar to previous findings in their studies, large longitudinal structures were observed in the central channel areas, and they focused their studies on the properties of these structures. Thirumaran et al. (2018) presented the analytical and numerical solution for abruptly stopped axial Couette flow. The stability analysis can be carried out to analyze the stability of the flow when a minor disturbance is introduced to the flow.

The perturbation theory has shown that the logarithmic law of velocity distribution is one of the theoretical results created to describe velocity profiles, which is essentially applicable to the overlap region less than 20% of the flow depth. Compared to the logarithmic law, the power law of velocity distribution, often provided by empirical methods, can be applied to a greater part of the flow domain. For the study of open-channel flows, the power law is usually considered a simple but completely empirical formula

for representing velocity profiles. The power law index of velocity can be analytically correlated with the Reynolds number and the equivalent roughness height. Still, it often appears to be related to the friction factor. The findings of this study have corresponded with the fact that one-sixth power is superior in engineering (Cheng 2007). Barenblatt and Prostokishin (1993) collected all of Nikuradse's (1932) classical data on velocity distribution and surface friction for comparison. The informative matching of the predictions to the experimental data indicates that the effect of molecular viscosity on the main body of fully developed shear flows essential, even at very high Reynolds numbers.

Maghrebi and Rahimpour (2005) presented a simple model for predicting isovel contours in ducts and open channels. They hypothesized that each element of the channel boundary would affect the arbitrary point velocity of the channel and then calculate the effect of the entire boundary by integrating on the wetted perimeter of the channel. In their paper, the logarithmic velocity distribution and power law were used to apply any other velocity distribution law. They used their model to calculate normalized isovel contours. Maghrebi (2006) presented a successful application of the Biot-Savart law in hydraulics. He used the similarities between the magnetic field of a wire current and the cross-section contours to obtain the pattern of velocity contours. A new approach has been developed based on harmonic mean distances to predict the dimensionless isovel contours in open channels with rectangular cross sections. The effects of free surface on the dimensionless isovel contours are investigated. Various combinations of free surface weight factor and aspect ratio simulate dimensionless isovel contours in rectangular cross sections. Discharge can be estimated based on a single point of velocity measurement and the dimensionless normalized isovels (Rahimpour 2017).

Study on the isovel contour in open channels and ducts has already been done in other researches, and examples of these studies have been provided. However, this paper uses a model previously proposed by Maghrebi and Givehchi (2010) to simulate downstream flow asymmetrically opening through a sluice gate across the river, isovel contour in channels whose walls move at equal velocities but different signs are produced and studied. For such studies, it is necessary to examine the flow between two infinite and parallel plates that move at equal velocities but opposite directions and called Couette flow. One of the aspects to be considered in such flows is the zero average discharge in the cross section. As the average discharge is zero, the average velocity will be equal to zero, leading to the creation of high-velocity contour lines on the sides near the moving walls. A distinctive aspect of the present work with the studies that Maghrebi and Givehchi (2010) conducted is that the channel bed on which the walls are placed is stable in this study.

2 Material and Methods

The most straightforward Couette flow is the flow between two infinite and parallel plates with b distance from each other, one of the walls being stable and the other wall moving at a constant velocity U. In this situation, Navier–Stokes equations are used to calculate the flow velocity profile. This Equation is as follows when the walls are on the left and right of flow (Munson et al. 2013):

$$u = \frac{1}{2\mu}\frac{\partial p}{\partial x}z^2 + c_1 z + c_2 \tag{1}$$

where z is the common location coordinate, and $u(z)$ denotes the velocity distribution. This equation indicates that the flow is one-dimensional. $(\partial p/\partial x)$ indicates the pressure gradient, and the c_1 and c_2 are the constants of the equation. Equation constants can be obtained by applying boundary conditions ($u=0$ at $z=0$, $u=U$ at $z=b$). Constants c_1 and c_2 are:

$$c_1 = \frac{U}{b} - \frac{b}{2\mu}\frac{\partial p}{\partial x} \tag{2}$$

$$c_2 = 0 \tag{3}$$

By placing c_1 and c_2 in Eq. (1), we have:

$$u = \frac{Uz}{b} + \frac{1}{2\mu}\frac{\partial p}{\partial x}\left(z^2 - bz\right) \tag{4}$$

Assuming the pressure gradient is zero $(\partial p/\partial x = 0)$, the only factor that drives the flow is the displacement of the right side of the moving plate at constant speed U, and Eq. (4) is simplified as follows. The flow velocity profile will be linear (Munson et al. 2013):

$$u = \frac{Uz}{b} \tag{5}$$

It should be emphasized that the following derivation is based on a channel with a flat bed. Couette flow fully developed when two walls are b apart from each other, and the left wall is fixed, and the right wall moves at constant velocity U, as shown in Fig. 1.

2.1 Cross-Sectional Isovel Contours

After examining the Couette flow between two infinite and parallel plates, where one of the walls is stationary, and the other is moving at a constant velocity U, a special condition of Couette flow between two infinite and parallel plates is examined in which two walls with constant velocity U move in opposite directions. As shown in Fig. 2,

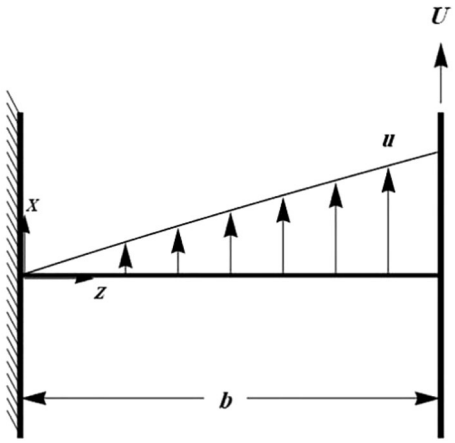

Fig. 1 Layer flow velocity profile between two infinite and parallel plates is stable, and the other is moving at a constant velocity U

the net average flow rate across any cross section is zero. Accordingly, the average velocity computed as $V=Q/A$ is zero, where A is the cross-section area. Therefore, the values of velocity contours in the channel section, obtained by dividing the point velocities by the average velocities, will be ambiguous and tend to infinity. For this situation, the velocity distribution is calculated from the following equation (Spurk 1997):

$$\frac{u(z)}{u_*} = \frac{1}{\kappa} \ln\left(\frac{bz}{b-z}\right) \tag{6}$$

where u_* is the shear stress, κ is the von Karman constant, 0.4 for clean water, b is the half distance between the two walls, z is the distance measured from the left wall, and ν is the kinematic viscosity of the fluid. The velocity distribution profiles of the turbulent Couette flow for different Reynolds numbers, indicated by relation ($\mathrm{Re} = 2bU/\nu$), can be obtained from:

$$\frac{u(z)}{U} = \frac{u_* 2b}{\nu} \frac{\nu}{2bU} \frac{1}{\kappa} \left[\ln\left(\frac{z}{2b}\right) - \ln\left(1 - \frac{z}{2b}\right)\right] \tag{7}$$

Equation (7) for the laminar and turbulent flow is plotted in Fig. 2. If the Reynolds number is less than 1500, the velocity distribution profile will be linear (Fig. 2a). The velocity distribution profile is nonlinear if the flow regime is disturbed (Fig. 2b). Figure 2a can also be plotted using the ($u = Uz/b$) relation.

The Couette flow is a hypothetical flow in which the role of the bed between two moving plates is not considered. However, such a flow can be quickly produced for a gas fluid that fills the space between two moving plates at the same velocities in different directions. But to produce a real flow of fluid between two plates, there is a need to have a stable bed. After discussing the relationship of the Couette flow between the two moving plates, it is now a situation that, in many aspects, is similar to the Couette flow between the two parallel plates but with differences. In addition to the sidewalls between two parallel plates in the Couette flow, there is also a stable bed, and practically the Couette flow between the two plates, changing to flow into a rectangular channel whose walls are at equal velocities and opposite directions.In this paper, it is assumed that each element of the channel boundary affects the arbitrary velocity point such as M in the cross section of the channel. Then the total boundary effects on arbitrary point M are obtained by integrating along the wetted perimeter of the cross section (Maghrebi and Rahimpour 2005). It was suggested that (Fig. 3):

$$u = \int_{\text{boundary}} c_1 f(r) \times ds \tag{8}$$

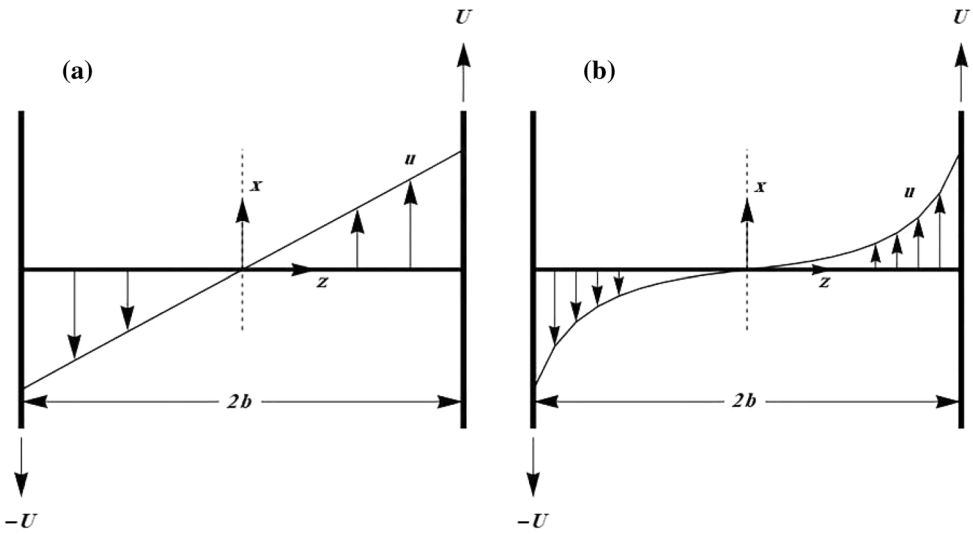

Fig. 2 Velocity distribution profiles for Couette flow as both walls move at a constant U speed **a** laminar flow and **b** turbulent flow

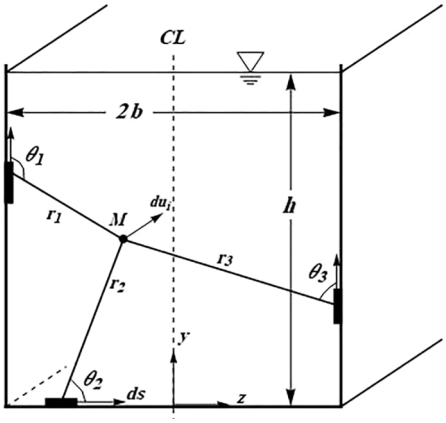

Fig. 3 The effect of boundaries on the velocity of the arbitrary point such as *M* at the channel cross section

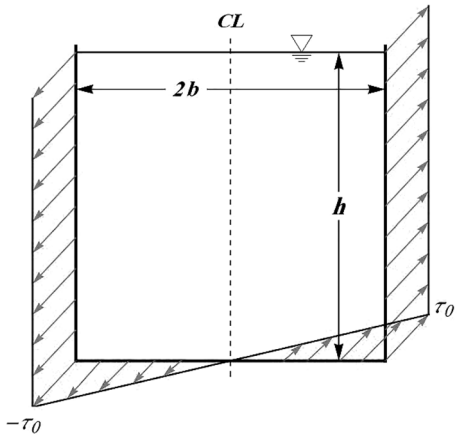

Fig. 4 Shear stress state in a rectangular channel with moving wall

where u is the streamwise velocity vector at a point in the cross section, $f(r)$ is the velocity function of the flow expressed on a flat plate with infinite width as a function of radial position, ds is an element of the wetted perimeter of the channel and c_1 is constants related to the roughness of the channel walls.

The velocity vector direction on the left side of Eq. (1) is the same as the multiplication vector direction () on the right side of the equation, which is perpendicular to the downstream flow section. The turbulent flow of a fluid into open pipes or channels can be estimated using the power-law velocity profile equation (Chen 1991):

$$\frac{u}{u_*} = c\left(\frac{y}{k_s}\right)^{\frac{1}{m}} \tag{9}$$

where u is the flow velocity, u_* is the shear velocity calculated from relation $(u_* = \sqrt{\tau_0/\rho})$, c is a constant that depends on Reynolds number, y is the vertical distance from the boundaries, and k_s is the height equivalent to the Nikuradse roughness and m, appearing in the power of Eq. (9), it varies between 4 and 12, depending on the turbulence (Yen 2002).

By replacing the radial distance r instead of the vertical distance y in Eq. 9, the following Equation will obtain (Maghrebi 2006):

$$f(r) = c_2 u_* r^{\frac{1}{m}} \tag{10}$$

where c_2 is a constant that depends on the nature of the flow; here, the nature of flow is related to the intensity of turbulence. So Eq. (8) will be as follows:

$$u(z,y) = \int_{\text{boundary}} c_1 c_2 \sin\theta u_* r^{\frac{1}{m}} ds \tag{11}$$

where θ is the angle between the position vector and the boundary element vector and $u(z, y)$ is the local point velocity at an arbitrary position of the channel section (Fig. 4).

It can be assumed that when the channel walls move at equal velocities but opposite directions, the shear stresses on the walls also have equal values but opposite signs. At the corners of the channel bed where the channel walls intersect with the bed, the shear stresses are precisely equal to the shear stresses on the walls. Still, since the shear stresses of the walls have opposite signs, at the channel bed, shear stresses also change from positive value to negative value. In this paper, the changes in shear stresses of the channel bed are considered linear. Therefore, the distribution of shear stresses of the bed changes linearly from $-\tau_0$ at the junction of the bed with the left side wall to τ_0 at the junction of the bed with the right sidewall.

3 Results and Discussion

Assuming linearity of shear stress variations in the channel bed, isovel contours can be obtained in such channels. Then perform simple but important analyzes of its various states. By performing these analyses, comparing the flow state in a channel whose walls are moving at equal velocities but opposite signs, with the flow condition in the channel with stable walls, can be done. Based on these comparisons, better decisions about the rivers with the reverse flow can be made. Figure 5 shows the status of the isovel contours in channels whose walls move at equal velocities but different signs for different width-to-depth ratios.

The nature of Couette flow is mainly related to the Reynolds number, which in turn related to the turbulent intensity. The flow is expected to be very turbulent when the channel walls move with equal velocities in opposite directions. By calculating the Reynolds number (Re=$\rho Ub/\mu$), it can be

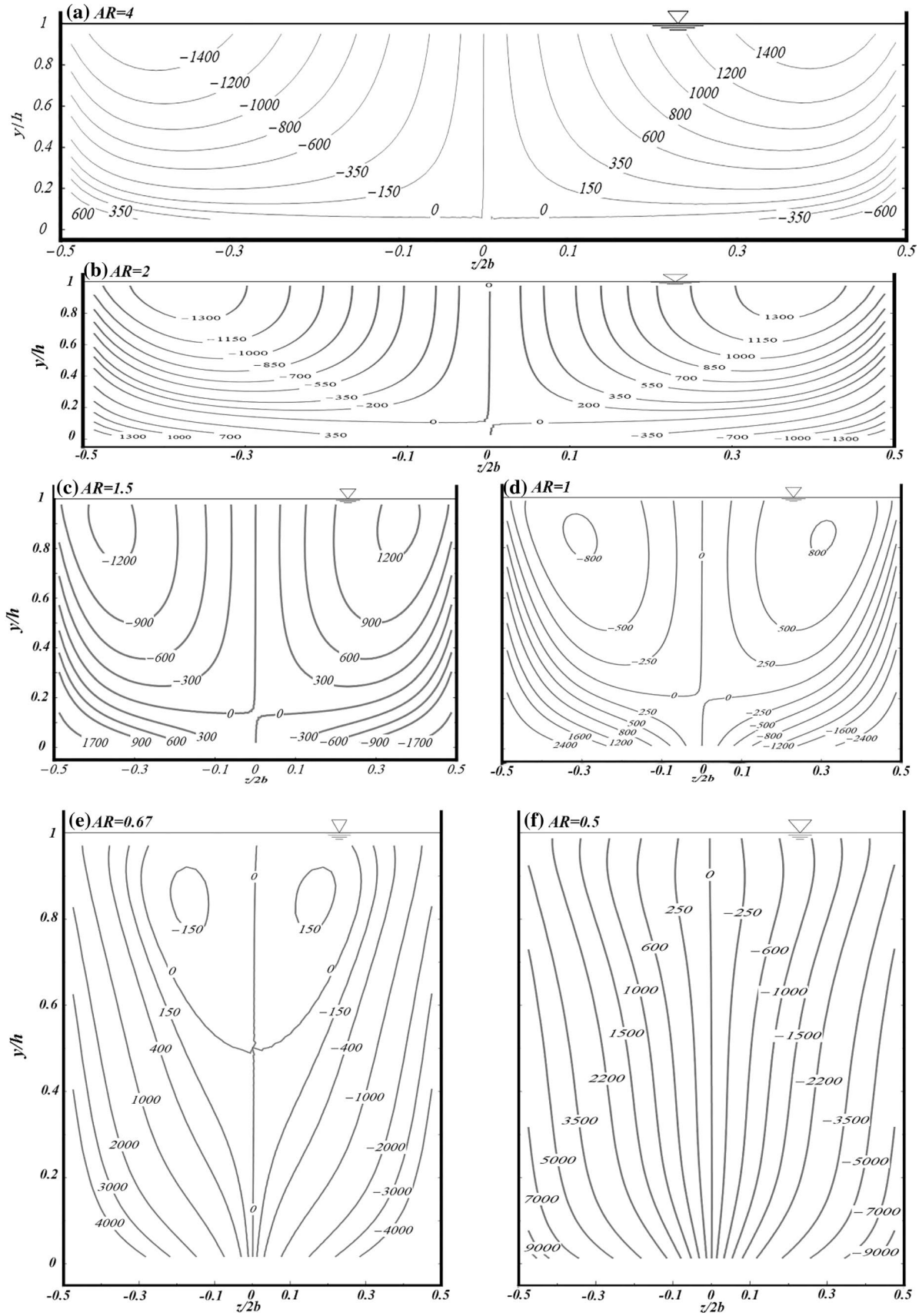

Fig. 5 Status of isovel contours for rectangular channels with moving walls for different width-to-depth ratios

seen that the Reynolds numbers are in the range of 2.5×10^5 and 2×10^6. Therefore, the flow regime will be fully turbulent. For specific aspect ratio AR=1, the following quantities have been adopted: b=0.5 m, U=1 m/s and $\nu=\mu/\rho=10^{-6}$ m^2/s. Also, it should be mentioned that the channel flow rate is zero for all aspect ratios.

Figure 5a shows isovel contours when the width-to-depth ratio of the channel is 4 for the channel whose walls are moving at equal velocities but with opposite signs. Because the velocities of the moving walls are equal but opposite, the average velocities at the section are very small and close to zero but never zero. Since the amount of isovel contours are obtained by dividing the point velocities by the average velocities, these contours have huge amounts. Since the velocities of the moving walls are equal but in opposite directions, in the middle of the channel width, the velocity contours are equal to zero. This zero boundary continues the middle of the channel width to walls. It intersects the wall with a 0.7 distance from flow depth to the flow surface. In this figure, the state of the isovel contours and direction of the velocity vector and water flow can be divided into four zones. These zones are pairwise symmetric, and their only difference is in the velocity vectors direction, but the velocity vectors are equal in the symmetric zones. Contours with a value equal to zero are the boundaries that divide the section into four zones. In this figure, the contours with the most values are near the flow surface. For example, the lowest point of velocity contours, which are -1400 and 1400, has 0.23 depths from the water surface, and their highest points are at the water surface. These contours also have 0.03 to 0.2 distance from the width of the section to the walls.

Figure 5b shows the state of the isovel contours where the width-to-depth ratio of the channel is 2. In this figure, the contours equal to zero forms the boundaries, which, as in the previous figure, divide the channel section into four zones. Because the effect of bed on shear stresses in this state is less than in the previous figure, the upper regions have a smaller area than Fig. 5a. These boundaries (contours of which are equal to zero) start from the channel walls and continue to the middle of the channel width and intersect the wall with a 0.57 distance from flow depth to the flow surface. Contours with 1300 are in the 0.05 to 0.2 channel width to the walls. The lowest point of these contours has a 0.15 depth distance from the flow surface, and the highest point is at the water surface. In this figure, contours with maximum values are in the bottom corners of the channel.

Figure 5c shows isovel contours when the width-to-depth ratio of the channel is 1.5. Contours with a value equal to zero are the boundaries that divide the section into four zones. These boundaries start from the channel walls and continue to the middle of the channel width, and at the point which is 0.43 flow depth below the flow surface, intersect the channel walls. It is also observed that the area of the upper regions is smaller than Fig. 5a, b because the effect of bed on shear stresses in this state is greater than in the previous figures. Contours with an amount of 1200 are in the range of 0.087 to 0.19 channel widths to the walls, and their lowest point is 0.25 channel depths away from the flow surface. Their highest point is at the surface of the flow. The contours with maximum amount are at the bottom corners and on both sides of the channel section and are 2100, but their velocity vectors have opposite directions. These maximum contours start from the channel wall and curve up to 0.05 channel widths to the walls.

Figure 5d shows the status of isovel contours when the width-to-depth ratio is 1. The zero boundaries, where the point velocities are equal to zero, divide the section into four symmetrically paired zones. Contours equal to zero continue from the walls to the center of the channel and reach the channel walls at the point of 0.43 flow depth below the flow surface. Since the channel bed effect is dramatic, the lower zero boundary regions have a larger surface area. The isovel contours form closed loops in the 0.07–0.25 depth range of the channel depth to the surface. Each of these closed loops is in the range of 0.15–0.24 channel widths to its walls. The point and mean velocities on the two sides of the zero boundaries in the middle of the channel are equal. Still, the velocity vectors on both sides of the boundary have opposite directions. So the only difference in the velocity contours around this boundary is their signs, and in Fig. 5e are shown the status of the isovel contours when the ratio of width to depth is 0.67; As can be seen, in the middle of the channel width, these contours are zero, and on both sides of the boundary, the values of these contours have large numbers because of very small mean velocities near zero. In this figure, the contours and directions of velocity vectors and water flow can be divided into four zones. These zones are pairwise symmetric, and their only difference is in the velocity vectors and water flow, but the value of velocity vectors is equal in the symmetric zones. Contours with a value equal to zero are the boundaries that divide the section into four zones. Velocity contours have maximum values at the top and bottom of these boundaries. The zero boundary of the left section at the flow surface is 0.23 channel widths from the left wall of the channel, and the zero boundary of the right channel is 0.23 channel widths from the right wall, indicating that the velocity contours are symmetric. According to the figure, the maximum velocity vectors are in the range of 0.08 to 0.23 flow depth from the water surface. We also have maximum velocity vectors at a distance slightly below zero boundaries. Because the channel height is relatively large to its width, the bed of the section has less impact on the upper regions, and the area of the upper regions of the zero boundary on both sides of the channel is smaller than the two lower regions.

The form of the isovel contours in Fig. 5f is different from the form of the isovel contours in the previous figures; the cause of this difference can be traced to the bed shear stresses. Given that the walls are moving at equal velocities but opposite directions, the point velocities are zero precisely in the middle of the channel. Thus, the values of the contours are equal to zero. Because the walls move in the opposite direction, velocity and flow vectors have opposite signs on both sides of the contour with a value equal to zero. Since these walls move at equal velocities, the amount of velocity vectors on both sides of the contour is zero and equal to each other. Because the bed shear stresses have less effect on the upper flow regions, the velocity contours are almost flat rather than curved lines. The effect of bed shear stresses on the flow in the lower corners of the channel is greater than in the upper regions of the channel section. For this reason, the values of velocity contours in the lower corners of the section are much larger than in the other regions of the channel.

Figure 6 is produced and plotted to compare the average depth velocities in open and closed channels when their walls move at equal velocities but different signs, better and faster.

In this figure, the highest rate of change is for the channel with a width-to-depth ratio equal to 0.5, which varies in the range of − 6000 to 6,000, and the lowest rate of change is for the channel with a width-to-depth ratio equal to 4, and it varies from − 200 to 200. Therefore, it can be concluded that the greater the width-to-depth ratio of the channel, the smaller the depth-averaged velocities due to the greater the effect of the channel bed on the velocity vectors at different points. Conversely, as the width-to-depth ratio becomes smaller, the effect of the channel bed section on the velocity vectors becomes smaller. Therefore, the depth-averaged velocities have larger values.

In Fig. 6, the graph indicated that solid triangles are for a closed rectangular channel with a width-to-depth ratio of 1 with walls moving at equal velocity and opposite directions to each other. In this case, in addition to changes in shear stresses of the bed, the changes in shear stresses of the channel roof also affect the amount of velocity vectors at different points in the channel; Therefore, the depth-averaged velocities, in this case, is smaller than in the open rectangular channel with the same width-to-depth ratio. In the above figure, the graph indicated with solid balls is for the depth-averaged velocities in the open channel and the width-to-depth ratio 1. It is observed that in this case, the depth-averaged velocities vary in the range of − 1500 to 1500, and the variation range of the closed rectangular channel with the width-to-depth ratio of 1 and the walls moving at equal velocities and opposite directions to each other are between − 700 and 700. Therefore, it can be concluded that the effect of channel roof shear stresses in closed rectangular channels with moving walls causes the depth-averaged velocities to be smaller.

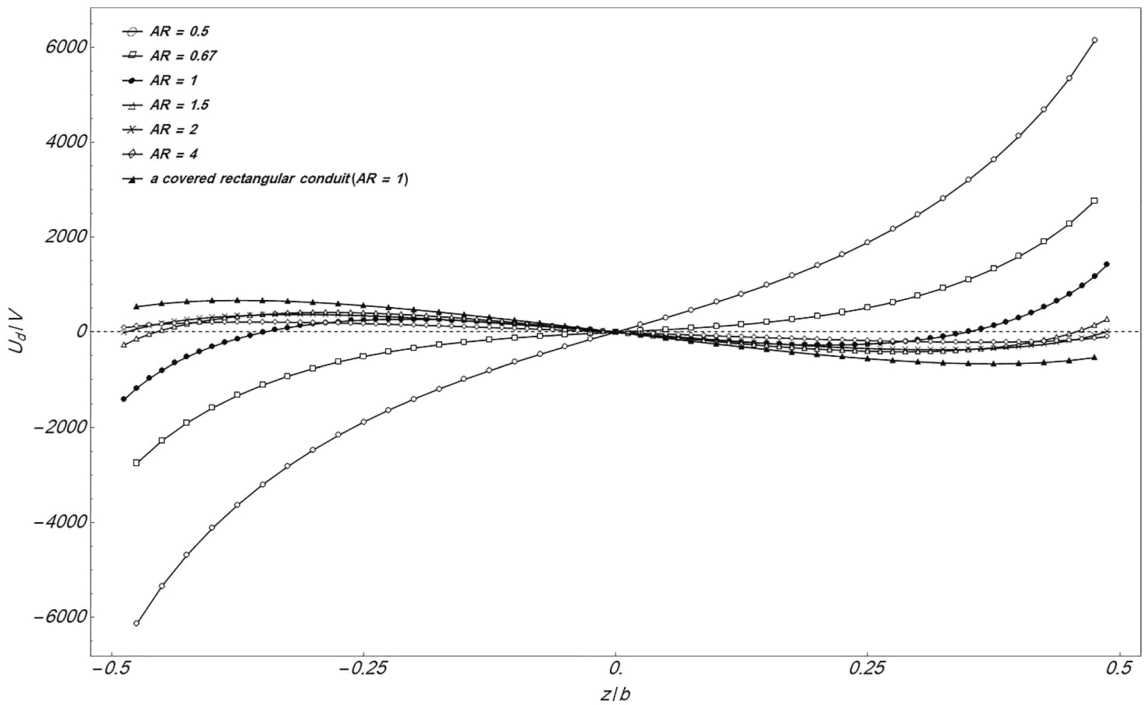

Fig. 6 The graph of average velocities variations in channels with moving walls for different width-depth ratios

The following figure shows the status of velocity contours in a closed channel, in which its width-to-depth ratio is one and its walls move at equal velocities but with different signs.

Due to the study that has already been conducted in this area, we know that for closed channels with stable walls, the velocity contours are concentric ellipses (Fig. 7a). In Fig. 7a, the values assigned to the contours are small because the walls are stationary, and the average velocities have much larger values than the average velocities when the walls move. Since in this study, the channel walls move at equal velocities but different signs, it is expected that the velocity contour with a value of zero will be formed exactly in the middle of the channel width and divide the section into two zones, which on both sides of this boundary, velocity vectors have opposite directions. As shown in Fig. 7b, on the two sides of the middle boundary of the channel section, the velocity contours are in the form of concentric ellipses, and there is a good match with the velocity contours when the walls are stable.

According to Figure 7b, the channel walls move with equal velocities but in opposite directions. Therefore, discharge through the cross section of the channel will be close to zero. Consequently, the average velocity of the flow passing through the channel cross section will be close to zero. Isovel contours are dimensionless and obtained by dividing point velocities by mean velocity. Given that the average speed is very close to zero, so the magnitude of isovel contours is very large.

4 Conclusion

The application of reverse flow is observed in many hydraulic phenomena; therefore, the study of reverse flow behavior is inevitable. For example, the asymmetric opening sluice gates in rivers (Maghrebi and Givehchi 2010) are simulated by moving walls. The hydraulic jump can be mentioned as a simple but widely used application of reverse flow. The upstream supercritical flow suddenly turns into the subcritical flow (Subramanya 2009). This phenomenon reduces

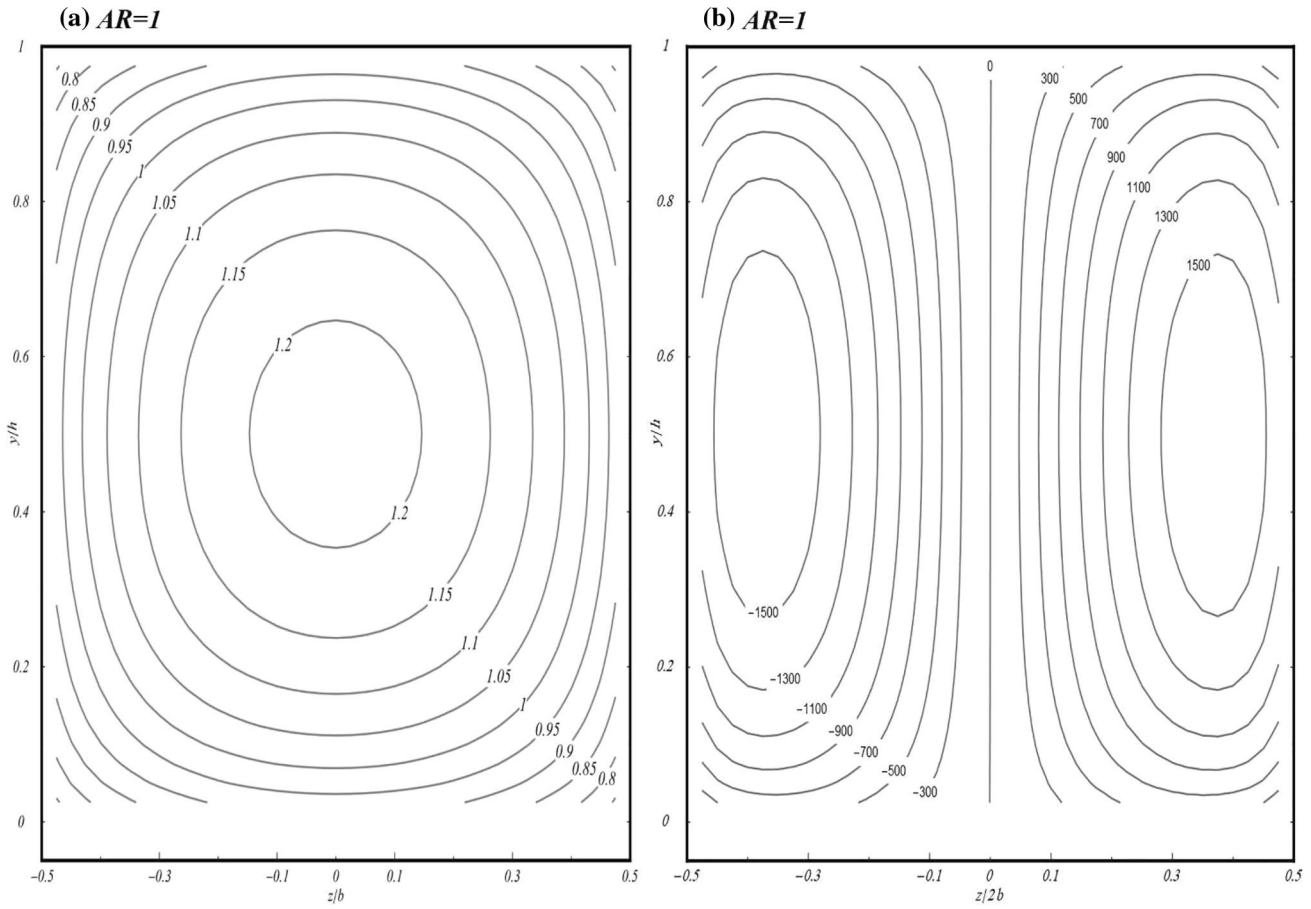

Fig. 7 The status of velocity contours in **a** duct and **b** closed rectangular channel with moving walls (the walls move at equal velocity and opposite direction)

water energy in the flow through dams, spillways, and other hydraulic structures. As a result, conducting studies on reverse flows can be useful and effective in maintaining hydraulic structures.

By studying the state of velocity contours in rectangular channels with walls moving at equal velocities but different directions, it is concluded that the shear stresses of the bed are the main cause of the difference of velocity contours in such channels with velocity contour in Couette flow between the two flat and parallel plates. As the width-to-depth ratio in the channel increases, the form of velocity contours in rectangular channels with walls moving at equal velocities, but different signs change more than the form of velocity contours in the Couette flow between the two flat and parallel plates. Suppose the walls move at equal and different velocities, both within the rectangular channel and between the two flat and parallel plates. In that case, a contour with zero value is formed precisely in the middle of the section width. The velocity contours in channels whose width-to-depth ratio is small will be very similar to the velocity contours of the Couette flow between the two parallel plates. But as the width-to-depth ratio increases, velocity contours change. As the width-to-depth ratio increases, the velocity contours change from straight and vertical to curved lines. The greater the width-to-depth ratio, the greater the radius of curvature of the velocity contours and in very high width-to-depth ratio change to straight horizontal lines. This also happens for contours with the zero value, and as the width-to-depth ratio increases, the contours with the zero value that are very small in width-to-depth ratios become curved lines. These contours can be the boundaries within the channel section, which are divided into four zones. Because the walls move at the same velocity, these areas are perfectly symmetrical. At small width-to-depth ratios, the two lower symmetric zones have a larger area of the channel section. As the width-to-depth ratio increases, the area of the lower regions will be smaller, and the area of the section that belongs to the upper symmetrical will be more significant. It is also observed that with decreasing width-to-depth ratios, the velocity and flow vectors directions are changing. At high width-to-depth ratios, the dominant flow direction on the right is downstream. In the lower two symmetric corners, we see the reverse flow, but in the small depth-to-depth ratios, the dominant direction on the right side of the section is upstream.

When the channel walls move at equal velocity but with different signs, the average discharge at the channel section is equal to zero; in this case, the average velocity will be zero. The velocity contours are also obtained by dividing the velocity vector by the average velocity; in this case, the velocity contours become ambiguous values. Their drawing would be practically impossible, but this article has shown that the average velocities will be small but never be zero. Therefore, velocity contours have a very large value and can be plotted.

References

Barenblatt GI, Prostokishin VM (1993) Scaling laws for fully developed turbulent shear flows. Part 2. Processing of experimental data. J Fluid Mech 248:521–529. https://doi.org/10.1017/S0022112093000874

Chen BC (1991) Unified theory on power laws for flow resistance. J Hydraul Eng 117:371–389. ©ASCE, ISSN 0733-9429/91/0003-0371

Cheng N (2007) Power-law index for velocity profiles in open channel flows. Adv Water Resour 30:1775–1784. https://doi.org/10.1016/j.advwatres.2007.02.001

Dey S, Barbhuiya AK (2005) Flow field at a vertical-wall abutment. J Hydraul Eng 131:1126–1135

Grosse S, Schröder W (2009) Wall-shear stress patterns of coherent structures in turbulent duct flow. J Fluid Mech 633:147–158. https://doi.org/10.1017/S0022112009007988

Hafeez HY, Ndikilar CE (2014) Flow of viscous fluid between two parallel porous plates with bottom injection and top suction. Prog Phys 10:49

Hamilton JM, Kim J, Waleffe F (1995) Regeneration mechanisms of near-wall turbulence structures. J Fluid Mech 287:317–348. https://doi.org/10.1017/S0022112095000978

Hu G, Yu L, Chen W, Hao J, Chu X (2016) Experimental and numerical investigations on the reverse flow phenomena in UTSGs. Prog Nucl Energy 92:147–154

Kitoh O, Nakabyashi K, Nishimura F (2005) Experimental study on mean velocity and turbulence characteristics of plane Couette flow: low-Reynolds-number effects and large longitudinal vortical structure. J Fluid Mech 539:199–227. https://doi.org/10.1017/S0022112005005641

Komminaho J, Lundbladh A, Johansson AV (1996) Very large structures in plane turbulent Couette flow. J Fluid Mech 320:259–285. https://doi.org/10.1017/S0022112096007537

Liu Y, Klaas M, Schröder W (2019) Measurements of the wall-shear stress distribution in turbulent channel flow using the micro-pillar shear stress sensor MPS3. Exp Therm Fluid Sci 106:171–182. https://doi.org/10.1016/j.expthermflusci.2019.04.022

Maghrebi MF (2006) Application of the single point measurement in discharge estimation. Adv Water Resour 29:1504–1514. https://doi.org/10.1016/j.advwatres.2005.11.007

Maghrebi MF, Givehchi M (2010) Discharge estimation in a tidal river with partially reverse flow. J Waterw Port Coast Ocean Eng 136:266–275

Maghrebi MF, Rahimpour M (2005) A simple model for estimation of dimensionless isovel contours in open channels. Flow Meas Instrum 16:347–352. https://doi.org/10.1016/j.flowmeasinst.2005.07.001

Munson BR, Okiishi TH, Huebsch WW, Rothmayer AP (2013) Fundamentals of fluid mechanics, 7th edn. Wiley

Nasif G, Balachandar R, Barron RM (2020) Supercritical flow characteristics in smooth open channels with different aspect ratios. Phys Fluids 32(10):105102. https://doi.org/10.1063/5.0021609

Orlandi P, Bernardini M, Pirozzoli S (2015) Poiseuille and Couette flows in the transitional and fully turbulent regime. J Fluid Mech 770:424–441. https://doi.org/10.1017/jfm.2015.138

Pereira AS, Mompean G, Thais L, Soares EJ (2017) Transient aspects of drag reducing plane Couette flows. J Nonnewton Fluid Mech 241:60–69. https://doi.org/10.1016/j.jnnfm.2017.01.008

Rahimpour M (2017) Dimensionless isovelocity contours in rectangular cross sections by harmonic mean distances. ISH J Hydraul Eng 23(3):241–245

Shinneeb AM, Nasif G, Balachandar R (2021) Effect of the aspect ratio on the velocity field of a straight open-channel flow. Phys Fluids 33:085110. https://doi.org/10.1063/5.0057343

Spurk J (1997) Fluid mechnics, problems and solitions. Springer, Berlin

Subramanya K (2009) Flow in open channels. Tata McGraw-Hill Education

Telbany MMME, Reynolds AJ (1980) Velocity distributions in plane turbulent channel flows. J Fluid Mech 100:1–29. https://doi.org/10.1017/S0022112080000973

Thirumaran V, Weliwita JA, Ishak MIM (2018) An analysis of axial Couette flow in annular region of abruptly stopped pipes. Phys Sci Int J 17:1–12

Yen BC (2002) Open channel flow resistance. J Hydraul Eng 128:20–39. https://doi.org/10.1061/(ASCE)0733-9429(2002)128:1(20)